

PHYSICAL REVIEW LETTERS

VOLUME 34

5 MAY 1975

NUMBER 18

$E \rightarrow B$ Structured Continuum in I_2

Joel Tellinghuisen

National Oceanic and Atmospheric Administration, U. S. Department of Commerce, Boulder, Colorado 80302
(Received 3 February 1975)

The recently reported structured continuum of the $E \rightarrow B$ transition in I_2 is analyzed to determine the E -state potential curve and the nature of the electronic transition moment. The minimum of the E curve lies at $41\,412\text{ cm}^{-1}$ with $R_e = 3.65 \pm 0.02\text{ \AA}$, and the dipole transition moment decreases with increasing R beyond $\sim 4\text{ \AA}$.

Rousseau and Williams¹ have recently described an experiment in which the E state of I_2 is excited by a sequential two-photon absorption process, $E \leftarrow B(0^+ \ ^3\Pi_u) \leftarrow X(0^+ \ ^1\Sigma_g)$. The single excited level then radiates to both bound and unbound levels of the B state, giving a spectrum which displays both discrete and diffuse features. The continuous segment of this spectrum shows structure characteristic of an "edge effect," or the existence of an extremum in the difference potential, $U_B(R) - U_E(R)$.^{2,3} This distinctive structure has been observed in a number of cases including one other transition in I_2 ,⁴ but none of the previously reported examples illustrates the phenomenon as simply as does the $E \rightarrow B$ spectrum of Rousseau and Williams. Because of its simplicity this case offers a valuable opportunity to demonstrate how information about the unknown potential curve and the transition-dipole-moment function can be deduced by synthesizing a spectrum which matches the experimental spectrum.

The emission process is illustrated in the potential diagram of Fig. 1. Excitation occurs from $v'' = 16, J'' = 15$ of the B state to $v' \approx 53$ of the E state.¹ The fluorescence intensity is governed mainly by the transition strength function and the Franck-Condon overlap. Interpreted classically the Franck-Condon principle dictates that the emission terminate on the dashed curve $V(R)$, which is the locus of points which conserve

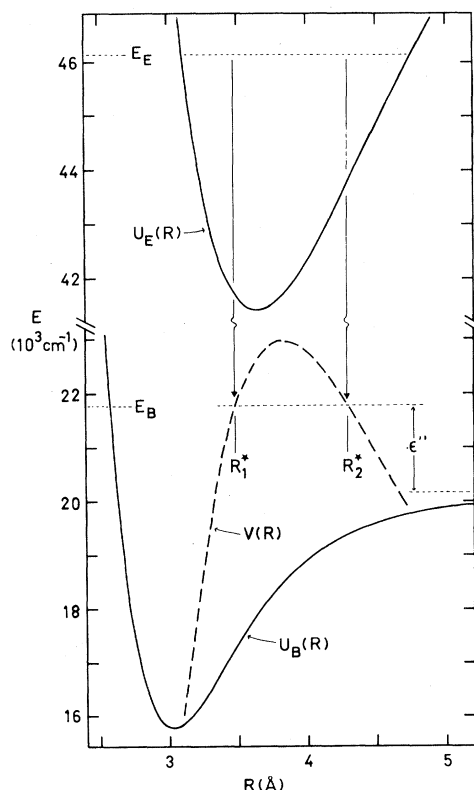


FIG. 1. Potential curves for E and B states of I_2 and difference potential $V(R) = U_B(R) - U_E(R) + E_E$ (energies relative to X -state minimum). Also shown are points of stationary phase for energy e'' above the B -state dissociation limit.

nuclear position and momentum in the transition. Of course the quantum mechanical overlap integrals are taken over all positive R . However, for a given B -state energy E_B the major contribution to the overlap occurs near R^* , the root of $V(R) = E_B$, where the E - and B -state vibrational wave functions have the same periodicity. If additionally the two wave functions are in phase at R^* , a spectral peak occurs at frequency $\nu = E_B - E_B$. For unbound B -state levels which lie below the extremum $V_{\max}(R)$, two regions of R contribute significantly to the overlap. These contributions may add constructively or destructively, and the result is the characteristic modulated interference pattern evident in the $E \rightarrow B$ diffuse spectrum. The remainder of this paper will concern just this portion of the $E \rightarrow B$ spectrum,

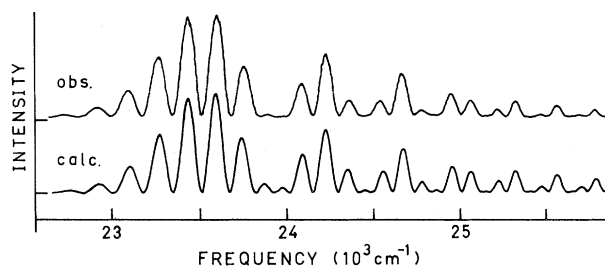


FIG. 2. Observed (from Ref. 1) and calculated $E \rightarrow B$ spectrum, continuous portion only.

which is reproduced together with the final calculated spectrum in Fig. 2.

The experimental spectrum is the sum of the R - and P -branch components, multiplied by a detector sensitivity function $F(\nu)$,⁴

$$S_{\text{obs}}(\nu) = F(\nu)\nu^5 \sum_{J''=J'+1} s(J', J'') |\langle \chi_{\epsilon'' J''} | \mu_e(R) | \chi_{\nu' J'} \rangle|^2. \quad (1)$$

Here $F(\nu)$ includes the explicit dependence on population and the fundamental constants, $s(J', J'')$ is the Hönl-London factor, and $\mu_e(R)$ is the transition moment function. $\chi_{\nu' J'}(R)$ and $\chi_{\epsilon'' J''}(R)$ are solutions to the radial Schrödinger equation (for effective potentials which include the centrifugal term), with $\chi_{\epsilon''}$ normalized to the density of states for energy ϵ'' . The frequency dependence in (1) includes a factor of ν^2 for monochromatic detection of quanta per unit wavelength interval. The application of (1) is straightforward when the potential curves and transition strength function are known. In the present case the problem of synthesizing a correct spectrum reduces to one of inferring the poorly known quantities, $U_E(R)$ and $\mu_e(R)$.

The semiclassical treatment of the integrals in (1) demonstrates clearly the origin of the interference effects in the spectrum.^{2,3,5-7} Away from the classical turning points the semiclassical wavefunctions can be represented (omitting normalization constants) as

$$\chi_{\nu'} \sim k_{\nu'}^{-1/2} \cos \varphi_{\nu'}, \quad \chi_{\epsilon''} \sim k_{\epsilon''}^{-1/2} \cos \varphi_{\epsilon''}, \quad (2)$$

where k is the local wave number and φ is the phase, i.e.,

$$k_{\epsilon''}^2 = 8\pi^2 \mu c [\epsilon'' - U_B(R)] / \hbar, \quad \varphi_{\epsilon''} = \int_{R_B}^R k_{\epsilon''} dR - \pi/4. \quad (3)$$

Here R_B is the classical turning point on the potential $U_B(R)$ for energy ϵ'' . The functional part of the Franck-Condon integrals is

$$\langle \chi_{\epsilon''} | \mu_e(R) | \chi_{\nu'} \rangle \sim \frac{1}{2} \int (k_{\epsilon''} k_{\nu'})^{-1/2} \mu_e(R) (\cos \varphi_+ + \cos \varphi_-) dR, \quad (4)$$

where $\varphi_{\pm} = \varphi_{\epsilon''} \pm \varphi_{\nu'}$. To evaluate this integral we invoke the stationary-phase approximation, which consists in recognizing that any significant contribution must come from a region of R where the phase (φ_+ or φ_-) is changing slowly with R , provided such a point exists. If $\mu_e(R)$ varies slowly with R , the condition for a point of stationary phase is $\partial \varphi / \partial R = 0 = k_{\epsilon''} \pm k_{\nu'}$. No such point occurs for φ_+ , and so the term involving $\cos \varphi_+$ contributes negligibly to the integral. For φ_- the condition is $k_{\epsilon''}(R^*) = k_{\nu'}(R^*)$, i.e., the Franck-Condon principle; and the points of stationary phase coincide with $V(R)$ in Fig. 1.

For E_B sufficiently below $V_{\max}(R)$ we may simply add the contributions to the integral from R_1^* and R_2^* , each evaluated in the conventional manner,⁷ obtaining

$$\langle \chi_{\epsilon''} | \mu_e(R) | \chi_{\nu'} \rangle \sim A_1 \cos(W_1 + \pi/4) + A_2 \cos(W_2 + \pi/4), \quad (5)$$

where

$$A_i = \mu_e(R_i^*) [k(R_i^*) | V'(R_i^*) |]^{-1/2}, \quad W_i = \int_{R_B}^{R_i^*} k_{\epsilon''} dR - \int_{R_E}^{R_i^*} k_{\nu'} dR. \quad (6)$$

Equation (5) can be written more illustratively:

$$\langle \chi_{e''} | \mu_e(R) | \chi_{v'} \rangle \sim 2A_1 \cos W_+ \cos W_- + (A_2 - A_1) \cos W_2 + \pi/4, \quad (7)$$

where $W_+ = (W_1 + W_2)/2 + \pi/4$ and $W_- = (W_1 - W_2)/2$. W_+ and W_- both vary smoothly with ϵ'' , so that when the second term in (7) is small, the spectrum has the appearance of a modulated sinusoidal function, $\cos^2 W_+ \cos^2 W_-$, with the second factor providing the envelope under which the first factor oscillates. Near $V_{\max}(R)$, where R_1^* and R_2^* coalesce, Eq. (5) becomes invalid.^{2,3} Nevertheless the qualitative picture presented by Eq. (7) remains valid, as is apparent in the spectra of Fig. 2.

Proceeding with the application of Eq. (1), we note that the $I_2 B$ state is well known spectroscopically,⁸ so that a reliable $U_B(R)$ can be constructed by use of the Rydberg-Klein-Rees method. Some information about the E state is available from studies of the $E \rightarrow B$ emission from low v' levels.^{9,10} Mulliken⁹ has considered two likely alternatives for the E -state electronic designation, $0^+ 1\Sigma_g^+$ and $0^+ 3\Pi_g^+$. Recent lifetime measurements by Wilkerson¹¹ yield $\tau(E) \approx 50$ nsec, supporting the latter choice. The vibrational analysis in Ref. 10 gave values for the electronic energy ($T_e = 41\,412$ cm⁻¹) and the first two vibrational constants ($\omega_e = 101.59$; $\omega_e x_e = 0.238$). On the basis of this information the excited level of Ref. 1 is found to lie between v' levels 52 and 53. Nothing is known about $\mu_e(R)$ from other sources. However, from an examination of the $E \rightarrow B$ spectrum in Ref. 1, it appears that $\mu_e(R)$ declines with R beyond ~ 4 Å: Without such decline the fluorescence near $26\,300$ cm⁻¹ would be much more intense, relative to that at lower and higher frequency, as these peaks result from very favorable Franck-Condon overlap between the large peak in $\chi_{v'}(R)$ near the right-hand turning point and corresponding regions of B -state wave functions near $v'' = 50$.

Lacking more definitive information about $U_E(R)$, I approximated this potential with a Morse curve based on the known ω_e and $\omega_e x_e$ values. Then with $\mu_e(R)$ taken as constant, R_e was varied to bring the calculated peaks into positional agreement with the observed peaks, while at the same time $\omega_e x_e$ was adjusted slightly to shift the calculated energy for selected v' levels into coincidence with the experimentally known excitation energy. Optimum agreement was obtained when the excited level was designated $v' = 52$ ($\omega_e x_e = 0.2200$) and R_e was ~ 3.65 Å. The functional form of $\mu_e(R)$ was then varied to reproduce the general intensity distribution of the experimen-

tal spectrum, with $F(\nu)$ taken as constant. The final calculated spectrum in Fig. 2 was obtained with $R_e = 3.649$ Å and $\mu_e(R) = 0.09/[0.09 + (R - 3.89)^4]$; J' was assumed to be 16.

The agreement between the spectra in Fig. 2 is convincing support for the general correctness of this analysis. The calculated spectrum is very sensitive to changes in $U_E(R)$; for example, changing R_e by only 0.001 Å significantly alters the intensity pattern. The spectrum is much less sensitive to changes in $\mu_e(R)$, as the main role of this quantity is to scale the overall intensity distribution. Since the detector sensitivity function was not determined in Ref. 1, the conclusions about $\mu_e(R)$ cannot be considered quantitative. In a rough sense the intensity at frequency ν reflects the square of $\mu_e(R)$ at $R_1^*(\nu)$ and $R_2^*(\nu)$; thus, for example, if $F(\nu)$ changes by a factor of 2 in the range $23\,500$ – $25\,500$ cm⁻¹, $\mu_e(R)$ would be in error by a factor of roughly 1.4 at 3.4 and 4.5 Å, relative to its value at ~ 3.9 Å. On the other hand, the qualitative behavior of $\mu_e(R)$ deduced here—particularly the significant decline beyond 4 Å—must be correct for any reasonable $F(\nu)$. This behavior is typical for transitions involving one ion-pair state [here the E state, which tends⁹ toward $I^+(^3P) + I^-(^1S)$], because the charge transfer is forbidden in the limit of large separation.

With allowance for the uncertainties in $\mu_e(R)$ and for deviations from the Morse form for $U_E(R)$, I estimate the derived value of R_e to be accurate within 0.02 Å. The true value of the vibrational quantum number for the excited level is likely within 1 of the derived value 52. The experiment of Ref. 1 provides no estimate of the magnitude of $\mu_e(R)$. However, from the 50-nsec lifetime¹¹ the peak transition moment appears to be close to the ~ 3 -D value estimated for the $I_2 D \leftrightarrow X$ transition.⁴

¹D. L. Rousseau and P. F. Williams, Phys. Rev. Lett. **33**, 1368 (1974).

²W. H. Miller, J. Chem. Phys. **52**, 3563 (1970).

³K. M. Sando, Phys. Rev. A **7**, 1889 (1973).

⁴J. Tellinghuisen, Chem. Phys. Lett. **29**, 359 (1974).

⁵F. H. Mies, J. Chem. Phys. **48**, 482 (1968).

⁶A. L. Smith, J. Chem. Phys. **49**, 4813 (1968).

⁷L. D. Landau and E. M. Lifshitz, *Quantum Mechanics—Non-Relativistic Theory* (Pergamon, London, England, 1958).

⁸J. Wei and J. Tellinghuisen, *J. Mol. Spectrosc.* **50**, 317 (1974).

⁹R. S. Mulliken, *J. Chem. Phys.* **55**, 288 (1971).

¹⁰K. Wieland, J. B. Tellinghuisen, and A. Nobs, *J. Mol. Spectrosc.* **41**, 69 (1972).

¹¹A. K. Wilkerson, private communication.

Coherence Measurement of Tensor Multipoles of Asymmetrically Excited Atomic States

D. A. Church, M. C. Michel, and W. Kolbe

Lawrence Berkeley Laboratory, Berkeley, California 94720

(Received 18 February 1975)

A specific coherence measurement technique is described, which yields the relative magnitudes of all predicted orientation and alignment parameters in tilted-foil-excited levels of ions and atoms. Quantum-beat frequencies and relative magnitudes are measured as a function of applied magnetic field strength and direction, and analyzed using Fano-Macek theory. The multipole moments of tilted-foil-excited 40-keV $^4\text{He } 4d \ ^1D_2$ atoms are measured and related to proposed excitation mechanisms.

Recently we observed coherence properties of asymmetrically excited atoms and ions via quantum beats in the optical decay radiation, when the uniformly moving particles were subject to an external uniform magnetic field oriented perpendicular to the beam direction.¹ Such beats also appear when the magnetic field is directed parallel to the ion beam.² We show here that measurements of the relative amplitudes of these quantum beats for *both* field directions, in linearly and circularly polarized light, completely define the relative magnitudes of the orientation and alignment tensors of the excited state. This technique is unambiguous, preserves the initial coherence, yields results with fractional percent precisions, and applies to any excited level.

Equations describing the polarization and static angular distribution of electric dipole radiation in terms of orientation and alignment tensor parameters have been given by Fano and Macek.³ In a uniform magnetic field, the predicted static radiation distribution is transformed to a time-dependent distribution by a coordinate rotation. The Fano-Macek theory is based only on the symmetry properties of the collision geometry, rather than on any specific properties of the interaction. Nevertheless, the initial analysis of our quantum-beat data¹ showed effects not predicted by their equations. We have since learned⁴ that one of Eqs. (18) of Ref. 3 is incorrect. An analysis of both original and new data, described below, is now in agreement with the corrected equations.

In terms of the orientation parameter O and the three alignment parameters A_0 , A_1 , and A_2 defined for the detection and collision reference frames, the corrected Eqs. (18) from Ref. 3 are

$$O_0^{\text{det}} = O_1^{\text{col}} \sin\theta \sin\varphi, \quad A_0^{\text{det}} = \frac{1}{2} A_0^{\text{col}} (3 \cos^2\theta - 1) + \frac{3}{2} A_{1+}^{\text{col}} \sin 2\theta \cos\varphi + \frac{3}{2} A_{2+}^{\text{col}} \sin^2\theta \cos 2\varphi,$$

$$A_{2+}^{\text{det}} = \frac{1}{2} A_0^{\text{col}} \sin^2\theta \cos 2\psi + A_{1+}^{\text{col}} \{ \sin\theta \sin\varphi \sin 2\psi + \sin\theta \cos\theta \cos\varphi \cos 2\psi \}$$

$$+ A_{2+}^{\text{col}} \{ \frac{1}{2} (1 + \cos^2\theta) \cos 2\varphi \cos 2\psi - \cos\theta \sin 2\varphi \sin 2\psi \},$$

where θ and φ are the polar coordinates of the light detector in a coordinate system which has as its \hat{z} axis the ion beam axis (see, e.g., Fig. 1 of Ref. 1). The orientation angle of a linear polarization analyzer relative to the \hat{z} axis is ψ . In our geometry, $\theta = \varphi = \pi/2$. If an external uniform magnetic field is applied, the multipole moments of the excited states precess in time t about the field direction at the Larmor frequency ω . For a field parallel to the beam direction \hat{z} , $\theta = \pi/2$ and $\varphi = \pi/2 + \omega t$, while a field perpendicular both to the beam and to the direction of light observation \hat{y} produces $\theta = \pi/2 + \omega t$ and $\varphi = \pi/2$. The expression for the optical decay light intensity [Eq. (14), Ref. 3] for circularly polarized light in a given transition is

$$I_{\text{cp}} = \frac{1}{3} CS \left[1 - \frac{1}{2} h^{(2)}(j_i, j_f) A_0^{\text{det}} + \frac{3}{2} h^{(1)}(j_i, j_f) O_0^{\text{det}} \right], \quad (1)$$

while the corresponding expression for linearly polarized light is

$$I_{\text{lp}} = \frac{1}{3} CS \left[1 - \frac{1}{2} h^{(2)}(j_i, j_f) A_0^{\text{det}} + \frac{3}{2} h^{(2)}(j_i, j_f) A_{2+}^{\text{det}} \right]. \quad (2)$$